PHYSICAL REVIEW B **80**, 081401(R) (2009)

Self-assembly of methanethiol on the reconstructed Au(111) surface

Georgi Nenchev,[1,*] Bogdan Diaconescu,[1] Frank Hagelberg,[2] and Karsten Pohl[1]
[1]*Department of Physics and Materials Science Program, University of New Hampshire, Durham, New Hampshire 03824, USA*
[2]*Department of Physics and Astronomy, East Tennessee State University, Johnson City, Tennessee 37614, USA*
(Received 22 April 2009; revised manuscript received 24 June 2009; published 3 August 2009)

We present a combined experimental and theoretical study of molecular methanethiol (CH_3SH) adsorption on the reconstructed Au(111) surface in the temperature range between 90 and 300 K in UHV. We find that the simplest thiol molecules form two stable self-assembled monolayer (SAM) structures that are created by distinct processes. Below 120 K, a solid rectangular phase, preserving the herringbone reconstruction, emerges from individual chains of spontaneously formed dimers. At higher adsorption temperatures below 170 K, a close-packed phase forms via dissociative CH_3SH adsorption and the formation of Au adatoms that are not incorporated into the SAM. We show that the combination of a strong substrate-mediated interaction with nondissociative dimerization and temperature activated removal of the Au(111) reconstruction drives the large-scale assembly of molecular CH_3SH into two distinct phases.

DOI: 10.1103/PhysRevB.80.081401 PACS number(s): 68.37.Ef, 64.75.Yz, 68.43.Bc, 68.43.Hn

Self-assembled monolayers (SAMs) are attracting substantial attention, fueled by the relative simplicity of their preparation, their structural integrity, and the ability to customize the layer by choosing an appropriate termination group.[1] These specific properties make SAMs suitable for nanotechnology applications such as surface customization, molecular electronics, and nanopattern creation.[2] Among the large variety of SAMs the self-assembly of alkanethiols ($CH_3(CH_2)_nSH$) on gold is probably the most studied.[1–3] Despite the large amount of data available, the exact nature of the bonding between the molecules and the surface is not completely determined.[4] The initial model of dissociative chemisorption of thiolates ($CH_3(CH_2)_nS$) at hollow sites in a $(\sqrt{3}\times\sqrt{3})R30°$ lattice[5] was challenged by experimental data,[6,7] which proposed the formation of thiolate disulfide on the surface by dimerization of the dissociated molecules. The dimerization mechanism and the bonding geometry are still extensively debated.[7–12]

For the adsorption of the simplest thiol molecule, CH_3SH on Au(111) only very recent observational[9,13–16] and theoretical[17,18] results are available. While desorption data seem still inconclusive,[9,13] initial scanning tunneling microscopy (STM) studies show the absence of self-assembly,[13] on-top adsorption at submonolayer (ML) exposures[14] without affecting the substrate reconstruction.[13] These results reveal that CH_3SH adsorption on Au(111) is substantially different from the larger alkanethiols, which form stable SAMs even at room temperature. The absence of self-assembly is attributed to the fact that CH_3SH lacks a hydrocarbon tail, which precludes the formation of ordered structures even at low temperatures. However, a very recent STM study revealed a continuous ordered structure.[16] At the same time a density-functional theory (DFT) calculation[18] proposed the possibility of dimerization of the nondissociated CH_3SH adsorbate on unreconstructed Au(111), driven by substrate-mediated charge exchange rather than van der Waals forces. In this Rapid Communication we show that CH_3SH not only spontaneously dimerizes on reconstructed Au(111) but also forms two stable continuous self-assembled structures.

The STM study is performed in an UHV chamber at a base pressure of 1×10^{-10} Torr, equipped with a homebuilt variable-temperature STM.[19] The (111) surface of the monocrystalline Au sample is prepared by sputter/anneal cycles. Methanethiol gas is delivered through a variable leak valve without further purification. The deposition is performed at a CH_3SH pressure of 5×10^{-8} Torr onto the cooled sample, and the STM images are taken at the same sample temperature within minutes.

Atomistic modeling of CH_3SH molecules in contact with the reconstructed Au(111) surface is performed using DFT within periodic boundary conditions as implemented in the *Vienna ab initio simulation package* (VASP).[20] The interaction of valence electrons and core ions is treated by the projector-augmented wave method,[21] involving a generalized gradient approximation to exchange and correlation in the framework of the Perdew-Wang 91 approach.[22] The wave functions are expanded in a plane-wave basis with an energy cutoff of 400 eV. The reconstructed Au(111) $22\times\sqrt{3}$ substrate is described by a four-layer slab, where the Au atoms in the top two layers are allowed to relax and those in the bottom layers are fixed in their bulklike structure. An energy cutoff of 0.1 meV was set for the respective geometry optimizations. The slabs are separated by a 10-layer-thick vacuum region. The Brillouin-zone integrations are carried out using the Monkhorst-Pack scheme in a $4\times1\times1$ mesh.[23] This approach is first applied to the pure reconstructed Au(111) $22\times\sqrt{3}$ surface. From this calculation, the amplitude of the periodic lateral displacement in the $\langle 11\bar{2}\rangle$ direction is determined to be 0.8 Å, which compares favorably with the STM result of approximately 0.9 Å.[24] For the corrugation amplitude in vertical direction an average of 0.125 Å is found, to be compared with the measured value of (0.16 ± 0.05) Å (Ref. 24) and a previous computational value of 0.12 Å.[25]

STM images taken after exposures of 0.5–1 L (10^{-6} Torr s) of CH_3SH at 100 K are presented in Figs. 1(a) and 1(b). Figure 1(a) shows that preferential adsorption takes place on the fcc areas and not on the hcp areas of the herringbone pattern. The ordering and period of the reconstruction network remain unchanged. The higher-resolution im-

 ©2009 The American Physical Society

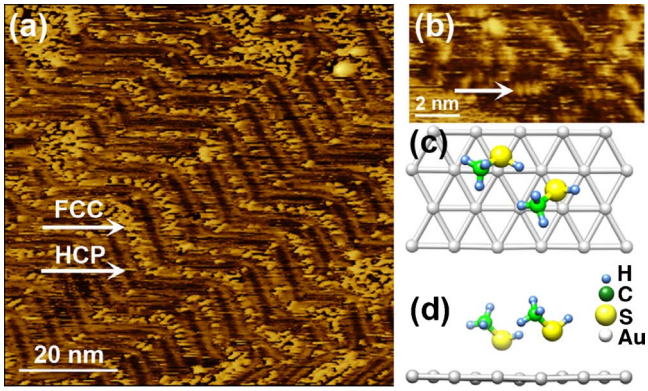

FIG. 1. (Color online) Sub-ML adsorption of CH_3SH on Au(111) at 100 K. (a) STM constant current image showing preferential adsorption on the fcc areas of the reconstructed substrate (U_{sample}=−1 V, I=3.1 nA). (b) Higher-resolution STM image, with arrow pointing at the dimer chains (−0.3 V, 1 nA). (c) Top view and (d) side view of the optimized DFT structures showing the shifted on-top/near-bridge adsorption sites.

ages of the disordered distinctive linear structures can be interpreted as a liquid phase proposed by Kondoh *et al.*[10] for low-coverage alkanethiol adsorption on Au(111). The distance between features, which our DFT calculations show to be CH_3SH dimers, measures (4.8 ± 0.4) Å along the chains; see Fig. 1(b). Further deposition saturates the fcc areas of the substrate and spilling over to hcp areas occurs.

At exposures of 1.5 L and substrate temperatures below 125 K we see a dramatic change in the ordering, as shown in Figs. 2(a) and 2(b). The substrate is now completely covered with domains of parallel rows of molecules, running normal to the Shockley partial dislocations. The structure has a rectangular unit cell of $(5.3 \pm 0.2) \times (14.4 \pm 0.4)$ Å^2. The STM line profile shown in the inset of Fig. 2(b) reveals a small individual height difference in the pairs of neighboring rows. The height of the molecules is (0.2 ± 0.07) Å. This solid phase is remarkably stable and exhibits few defects.

After deposition of 2 L CH_3SH at 160 K, a continuous ordered phase appears (see Fig. 3). This SAM has a hexagonal unit cell with a nearest-neighbor distance of (5.1 ± 0.5) Å and no height variation between the individual molecules, as shown in Fig. 3(b) and the line profile in the top inset of Fig. 3(a). The herringbone reconstruction is lifted and ML-thick gold adislands are visible underneath the SAM; see line profile in the bottom inset of Fig. 3(a). In all three observed structures CH_3SH molecules desorb above 200 K and lead to a recovery of the clean reconstructed gold substrate. A transition from one phase to the other is not observed, neither by exposure nor temperature variation.

To obtain fundamental insight into the origin of the two distinct SAM phases, we performed a DFT calculation of the bonding geometry and binding energy of CH_3SH adsorption on reconstructed Au(111) at T=0. Two CH_3SH molecules are attached to the fcc domain of the substrate, as obtained from our optimization of the pure reconstructed Au(111) surface. The initial positions of the adsorbates were chosen in accordance with the observation that a single CH_3SH molecule binds preferentially in the fcc hollow region with a tendency

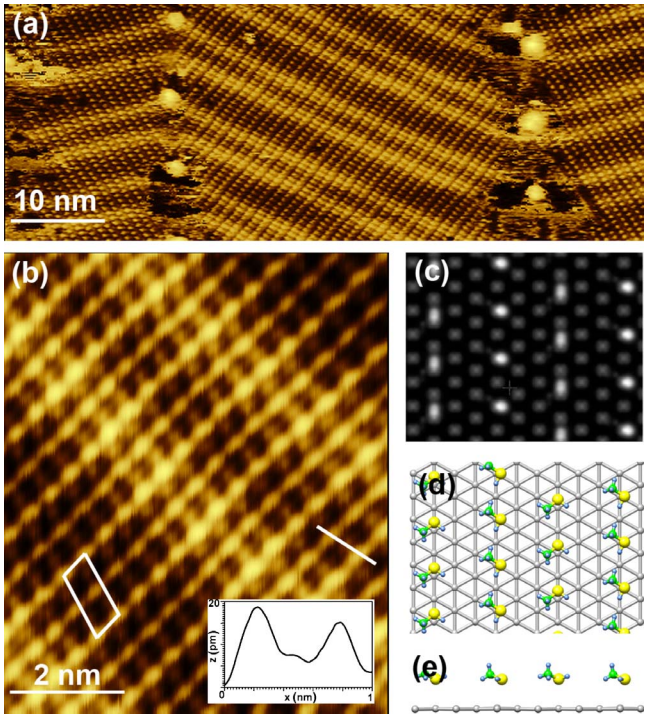

FIG. 2. (Color online) (a) Large scale (−1 V, 0.3 nA) and (b) high-resolution (−0.4 V, 0.3 nA) STM images of the solid phase of CH_3SH self-assembled on reconstructed Au(111) at 110 K. (a) The herringbone pattern is visible as a corrugation of the film along with clusters decorating the threading dislocations, while (b) is showing the unit cell and a line profile along the white line in the inset. (c) Calculated electronic density between E_F and E_F+2.0 eV for the optimized structure. (d) Top view and (e) side view of the optimized DFT adsorption structure showing the zigzag arrangement of alternating shifted-bridge and shifted-top sites in the long direction of the observed $(3\sqrt{3} \times 2)$ unit cell of the SAM.

toward an on-top site.[17] Also, acknowledging that the *S*-*S* equilibrium distance between adjacent CH_3SH molecules tends to exceed the distance between adjacent equivalent sites,[18] we chose the initial *S*-*S* distance as 3.2 Å and thus slightly larger than the separation between closest Au atoms. Optimization yields an equilibrium structure at an increased *S*-*S* distance of 4.0 Å, and with an adsorption energy E =0.89 eV, where E is defined as the energy release per molecule upon attaching two CH_3SH molecules to the Au(111) $22 \times \sqrt{3}$ unit cell. In this final geometry, one of the two paired molecules moves from its original position toward a bridge site, and the other toward an on-top site, as shown in Figs. 1(c) and 1(d). To assess the stability of this phase, we carried out a further computation for two CH_3SH molecules at fcc sites with an initial *S*-*S* distance of 5.1 Å. This value remains nearly unaffected in the course of geometry optimization, indicating negligible mutual influence of the two molecules on each other. Therefore, the adsorption energy difference between both situations may be used as a measure for the interaction strength between the paired adsorbates. That difference is 0.1 eV in favor of the configuration at an equilibrium *S*-*S* distance of 4.0 Å, significantly larger than estimated van der Waals effects.[26] Our computations show that the dimer phase impacts the geometry of the substrate by

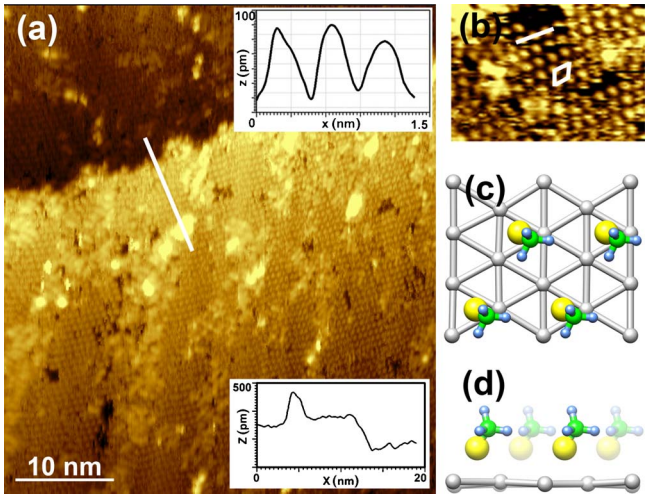

FIG. 3. (Color online) (a) STM image of the hexagonal phase covering both sides of a terrace edge on Au(111) (−3.1 V, 0.5 nA). (b) Higher-resolution image showing the $(\sqrt{3}\times\sqrt{3})R30°$ unit cell (−0.4 V and 0.3 nA). (c) Top view and (d) side view of the optimized DFT model structure showing the shifted-top-bridge adsorption geometry (Ref. 18). The top and bottom insets in (a) are line profiles corresponding to the white line in (b) and in (a), respectively.

decreasing the corrugation amplitude by 30% without lifting the reconstruction.

High-resolution STM images of the rectangular solid phase seen at high coverage [Fig. 2(a)] can be explained by a DFT-based model that is comprised of nondissociated molecules ordered in a $(3\sqrt{3}\times 2)$ lattice. While the low-coverage precursor phase of individual dimer chains forms by spontaneous dimerization of CH_3SH molecules the details of the transition to this SAM structure could not be observed. However, our results strongly suggest that the spontaneous change in the adsorption geometry is driven by intermolecular interactions. The bonding geometry is different from the one proposed earlier[16] as the molecular rows are bonded iteratively to shifted-bridge and shifted-top sites in zigzag orientation, as shown in Figs. 2(d) and 2(e). From extensive DFT optimization, this geometry has an energy advantage of 57 meV over a structure comprised of straight parallel adsorbate rows in the $\langle 1\bar{1}0\rangle$ direction where the CH_3SH molecules tend to bond toward on-top sites, maintaining largely the orientation with respect to the surface as shown in Fig. 2(d). The zigzag and the on-top geometry, which emerges from the structure displayed in Figs. 2(d) and 2(e) by mapping the bridge sites onto the adjacent on-top sites in the $\langle 11\bar{2}\rangle$ direction, are separated by a margin of 3 meV per molecule. Considering the impact of thermal and dispersion effects which are not included in the DFT method employed here, this difference is too small to allow for a statement with respect to the relative stability of the two compared configurations. However, the experimental evidence in favor of the zigzag model is unambiguous.

The experimental conclusions point at a charge-based interaction as the leading contributor for the phase formation for the following reasons: (i) the solid phase can be imaged at voltages well above the established dissociation barrier of the CH_3SH molecule of −2.5 V (Ref. 14) with no impact to the film; and (ii) exposures above 1.5 L do not change the structure of the film, so once created the ML completely passivates the surface. Moreover, in Fig. 2 we shall notice that the iterative height of the neighboring rows is not switching when the rows cross from fcc to hcp area, so the height alternation is not due to the substrate reconstruction.

The nearest-neighbor distance of (5.1 ± 0.5) Å in the hexagonal phase [Fig. 3(b)] is consistent with the theoretical value of 4.99 Å for a $(\sqrt{3}\times\sqrt{3})R30°$ primitive cell of close-packed and out-of-plane oriented molecules depicted in Figs. 3(c) and 3(d). For longer alkanethiols at saturation coverage this orientation is predominant, and is referred to as the ϕ phase.[27] The out-of-plane orientation is supported by the measured elevation of 0.8 Å of the film with respect to the substrate, four times the elevation of the solid phase. Moreover, the out-of-plane monomer phase has been identified earlier as the most stable equilibrium geometry of 1 ML thiolate on Au(111).[18] The presence of one-atomic-layer-thick Au clusters of about 2–3 % coverage along with the absence of the herringbone dislocation network, as seen in Fig. 3(a) and the line profile in the bottom inset, are consistent with the established scenario of dissociative bonding.[11,28] In this model CH_3SH molecules react with the reconstructed Au(111) surface by pulling out gold atoms to eliminate the herringbone dislocations and by bonding as thiolate to the dislocation-free Au(111) surface. Moreover, the total coverage of the uniformly distributed Au adclusters of about 0.02 to 0.03 ML is consistent with the number of excess Au atoms in the reconstructed (111) surface. These observations clearly suggest that this SAM phase does not require individual Au adatoms to participate in the molecular bonding [Figs. 3(c) and 3(d)]. The phase formation can be attributed to the increased diffusion of gold atoms at 160 K. The elevated formation temperature, the unit-cell size variation, and the abundance of defects in the film all suggest that the intermolecular interaction is much weaker than in the case of the solid phase. Considering the weak substrate bonding close to the desorption temperature a delicate balance is required for this phase to form. The failure to observe a transition between the two compact phases can be attributed to the fact that the activation barrier for such transition lies above the desorption energy, in agreement with previous results.[13,17]

In this study we presented the distinct processes that are driving the formation of the two methanethiol SAM structures on Au(111): (i) spontaneous dimerization of CH_3SH molecules precedes the formation of the solid rectangular SAM phase at $T\leq 125$ K on herringbone reconstructed Au(111), and (ii) dissociative CH_3SH adsorption at 150 K $\leq T\leq 170$ K causes the creation and diffusion of Au adatom and thus removal of the herringbone reconstruction and drives the formation of the closed-packed SAM structure or ϕ phase. The coexistence of dislocation network and dimer chains is confirmed by DFT calculations. The remarkable stability of the solid phase is attributed to the unusual strength of the substrate-mediated interaction and is a specific property of CH_3SH self-assembly.

This work was supported in part by the National Science Foundation under Grant No. DMR-0134933 and by the Nanoscale Science and Engineering Center for High-rate Nanomanufacturing (Grant No. NSEC-425826). The computations were performed on the CRAY XT3 machines Sapphire at the U.S. Army/Engineer Research and Development Center (ERDC, Vicksburg, MS) and Bigben at the Pittsburgh Supercomputer Center, in collaboration with Jackson State University, and supported by the DoD through Contract No. W912HZ-06-C-005. The help of Jianhua Wu in preparing some of the figures is acknowledged.

*Present address: Logic Technology Development Group, Intel Corporation, Hillsboro, OR 97124. georgi.nenchev@unh.edu

[1] A. Ulman, *Self-Assembled Monolayers of Thiols* (Academic Press, San Diego, 1998).

[2] H. Nalwa and R. Smalley, *Encyclopedia of Nanoscience and Nanotechnology* (American Scientific Publishers, Valencia, CA, 2002).

[3] G. E. Poirier, Chem. Rev. (Washington, D.C.) **97**, 1117 (1997).

[4] M. Biener, J. Biener, and C. Friend, Surf. Sci. **601**, 1659 (2007).

[5] G. E. Poirier, M. J. Tarlov, and H. E. Rushmeier, Langmuir **10**, 3383 (1994).

[6] P. Fenter, A. Eberhardt, and P. Eisenberger, Science **266**, 1216 (1994).

[7] M. Roper, M. Skegg, C. Fisher, J. Lee, V. Dhavak, D. Woodruff, and R. Jones, Chem. Phys. Lett. **389**, 87 (2004).

[8] R. Staub, M. Toerker, T. Fritz, T. Schmitz-Hübsch, F. Sellam, and K. Leo, Langmuir **14**, 6693 (1998).

[9] G. Liu, J. Rodriguez, J. Dvorak, J. Hrbek, and T. Jirsak, Surf. Sci. **505**, 295 (2002).

[10] H. Kondoh, C. Kodama, H. Sumida, and H. Nozoye, J. Chem. Phys. **111**, 1175 (1999).

[11] P. Maksymovych, D. C. Sorescu, and J. T. Yates, Phys. Rev. Lett. **97**, 146103 (2006).

[12] R. Mazzarello, A. Cossaro, A. Verdini, R. Rousseau, L. Casalis, M. F. Danisman, L. Floreano, S. Scandolo, A. Morgante, and G. Scoles, Phys. Rev. Lett. **98**, 016102 (2007).

[13] I. I. Rzeznicka, J. Lee, P. Maksymovych, and J. Yates, Jr., J. Phys. Chem. **109**, 15992 (2005).

[14] P. Maksymovych, D. Sorescu, D. Dougherty, and J. Yates, Jr., J. Phys. Chem. B **109**, 22463 (2005).

[15] B. Diaconescu, G. Nenchev, J. Jones, and K. Pohl, Microsc. Res. Tech. **70**, 547 (2007).

[16] P. Maksymovych and D. Dougherty, Surf. Sci. **602**, 2017 (2008).

[17] J.-G. Zhou and F. Hagelberg, Phys. Rev. Lett. **97**, 045505 (2006).

[18] J.-G. Zhou, Q. L. Williams, and F. Hagelberg, Phys. Rev. B **76**, 075408 (2007).

[19] B. Diaconescu, G. Nenchev, J. de la Figuera, and K. Pohl, Rev. Sci. Instrum. **78**, 103701 (2007).

[20] G. Kresse and J. Furthmüller, Phys. Rev. B **54**, 11169 (1996).

[21] P. E. Blöchl, Phys. Rev. B **50**, 17953 (1994).

[22] J. P. Perdew, J. A. Chevary, S. H. Vosko, K. A. Jackson, M. R. Pederson, D. J. Singh, and C. Fiolhais, Phys. Rev. B **46**, 6671 (1992).

[23] H. Monkhorst and J. Pack, Phys. Rev. B **13**, 5188 (1976).

[24] J. V. Barth, H. Brune, G. Ertl, and R. J. Behm, Phys. Rev. B **42**, 9307 (1990).

[25] Y. Wang, N. S. Hush, and J. R. Reimers, Phys. Rev. B **75**, 233416 (2007).

[26] For assessing the possible impact of the van der Waals force on the order of stabilities among the two configurations, we investigated the interaction between the pure thiol molecules in both configurations (Ref. 29) and subjected both systems to DFT and *ab initio* analysis at the B3LYP/6-311G and MP4/6-311G levels, respectively. The latter method, in contrast to DFT based procedures, is an adequate choice for the treatment of van der Waals interactions as Møller-Plesset perturbation theory describes dispersion phenomena well (Ref. 30). The van der Waals component is estimated by evaluating the difference $(E^{MP4}-E^{B3LYP})[d(\mathrm{SS})=5.0\ \text{Å}]-(E^{MP4}-E^{B3LYP})[d(\mathrm{SS})=4.0\ \text{Å}]$. The result is 28 meV, which is substantially lower than the energy difference between the two compared adsorption geometries. This finding confirms that the dimerization described here is a surface assisted rather than an intermolecular effect.

[27] G. Poirier, Langmuir **15**, 1167 (1999).

[28] P. Fenter, F. Schreiber, L. Berman, G. Scoles, P. Eisenberger, and M. Bedzyk, Surf. Sci. **412-413**, 213 (1998).

[29] M. Frisch *et al.*, *Gaussian 03, Revision C.02* (Gaussian Inc., Wallingford, CT, 2004).

[30] C. Tuma and J. Sauer, Phys. Chem. Chem. Phys. **8**, 3955 (2006).